Journal of Polymers and the Environment (2024) 32:1122–1134
https://doi.org/10.1007/s10924-023-03021-7

RESEARCH

Recycling ABS from WEEE with Peroxo-Modified Surface of Titanium Dioxide Particles: Alteration on Antistatic and Degradation Properties

Iago. M. Oliveira[1] · Jessica C. F. Gimenez[2] · Gabriela T. M. Xavier[3] · Marco A. B. Ferreira[2] · Caio M. P. Silva[2] · Emerson R. Camargo[4] · Sandra A. Cruz[2]

Accepted: 3 August 2023 / Published online: 22 August 2023

Abstract

The increasing concern about plastic disposal and its impact on the environment has led to the necessity to reuse these materials, completing their life cycle within the circular economy mentality: production, use, recycling, and reuse. One of the residues that has caused great concern is the so-called waste electrical and electronic equipment (WEEE). The reintroduction of a recycled material back into the market requires some type of modification since the recycling process lightly alters the general properties of those materials. In this work, we studied the recycling of ABS—one of the polymers most found in waste electrical and electronic equipment—and its modification through commercial titanium dioxide (TiO_2) and modified with peroxide groups (TiO_2–OPM). The TiO_2–OPM have interesting electrical properties due to their lower band gap values, which results in them being good candidates for the modification of recycled polymers for WEEE applications. For this, different percentages of particles were incorporated into ABS from the electro-electronic industry. Aspects of degradation, rheology, and antistatic were analyzed. A good interaction between the particle and polymer is observed, especially for those modified with the peroxo group. Nevertheless, it is observed that this modification promotes a reduction in the initiation of exothermic reactions for the butadiene phase, which seems to be a positive aspect because it preserves the acrylonitrile-styrene phase. The interaction is observed rheologically, indicating the formation of a percolated network that favors antistatic characteristics, even with a reduced amount of TiO_2-OPM. This work presents a framework for the development of more sustainable materials with concepts of a circular production system.

✉ Sandra A. Cruz
sandra.cruz@ufscar.br

[1] São Carlos Institute of Chemistry (IQSC), University of São Paulo (USP), São Carlos, Brazil

[2] Department of Chemistry, Exact Sciences and Technology Centre (CCET), Federal University of São Carlos (UFSCar), Rodovia Washington Luís, Km 235, 10 SP-310, São Carlos, Brazil

[3] Center of Natural and Human Sciences, Federal University of ABC (UFABC), Av. Dos Estados, 5001, Santo André 09210-580, Brazil

[4] Interdisciplinary Laboratory of Electrochemistry and Ceramics (LIEC)Department of ChemistryExact Sciences and Technology Centre (CCET), Federal University of São Carlos (UFSCar), São Carlos, Brazil

Graphical Abstract

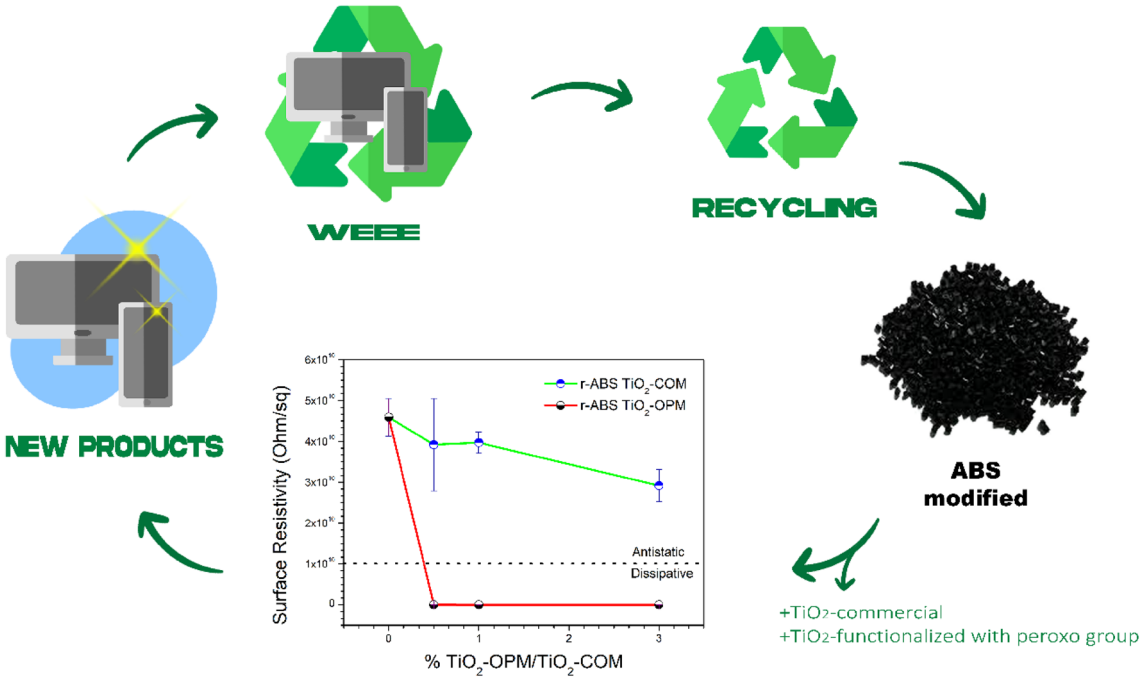

Keywords Recycled ABS · Modified surface titanium dioxide · Waste from electrical and electronic equipment · Electrostatic discharge protection · Dissipative composites

Introduction

It is safe to say that nowadays polymer production has surpassed all other man-made materials. Since the beginning of the commercial interest in these so-called plastics, way back in the 1950s, a vast diversity of applications has been found [1]. One of the most common uses of these materials lies in their application as electronic equipment enclosures, such as those used for computers and cell phones [2]. From this emerges a growing problem related to the final destination of that equipment when they reach the end of their optimal operational lifespan. The electronic industry has lived through several technological revolutions these past decades. The constant evolution of technology coupled with a planned obsolescence of products leads to a huge amount of waste electrical and electronic equipment (WEEE) [3].

Plastics take up differentiated proportions in WEEEs, accounting for a wide range of 3.5–45.0% in mass, according to data from 2022 [4]. Of all polymers contained in the WEEE, the ABS (acrylonitrile butadiene styrene) polymer represents one of the largest constituents by a mass fraction, being responsible for more than a third of the plastic content found in this type of waste [5, 6, 8]. Reintroducing the polymers contained in WEEE into the production chain and the market is a recurring theme in the literature [7–11], and many companies in the sector are aiming to develop polymers with properties similar to or even superior to those of pristine material. This brings forth the concept of a circular economy with a concern for the environmental effects of these materials and their manufacturing processes. A closed-loop or circular production system is known as Cradle to Cradle (C2C) and it offers an opportunity to radically revise the current take-make-waste system of production [12]. The purpose of C2C for the construction environment is to encourage smart designs that have a positive synergistic interaction with the natural world. This philosophy is a novel paradigm used to model products and services that are advantageous in terms of economic, well-being, and environmental sustainability to establish a tenable world [13]. Therefore, these concepts make us think about the advantages and sustainable values of recycled polymer modification and reintroduction back into the market. The function of an enclosure is to ensure protection for electronic equipment, not only physically but also to protect its internal electrical components against electrostatic discharges and so it needs to present certain conditions [14]. Knowing the polymers' inherently insulating characteristics represents the need to modify these materials so that they can be used as electronic equipment enclosures. One

way to modify the polymer's properties lies in the making of composites through the insertion of adequate particles and, thus, the enhancement of the target properties [15]. For this application, an increase in surface conductivity is required, which can mitigate eventual electrical discharges [16]. The choice of an adequate particle lies in its properties, so when mixed with the polymer, the composite will acquire and show some of the particle's properties. Recent work shows that the peroxo group modified TiO_2 particles can be viewed as good candidates for polymer modification. These particles have good photocatalytic properties, as Nogueira et al. showed [17]. They also have interesting electrical properties due to their lower band gap values, as presented in Francatto's work [23]. These results indicated that the incorporation of those particles into a polymeric matrix could be a means of improving or adding some desired functionalities.

However, despite the numerous works presented in the literature on WEEE-based ABS recycling, there are no studies on the association between the promising properties of the TiO_2-OPM particles and the system's potential upcycling. Therefore, to enhance the conductive behavior of the r-ABS, the peroxo group modified-surface titanium dioxide (TiO_2-OPM) is a possibility. Based on its calculated band gap value [23], it was hypothesized that this material could present a potentially better electrical property compared to commercial TiO_2 and the resulting recycled ABS/TiO_2-OPM composite would become a dissipative material, showing a good capacity to prevent an electrostatic discharge event.

Therefore, this work aimed to modify a WEEE-originated recycled ABS polymer matrix, producing a composite with the mixture of this polymer and the TiO2-OPM particles. The resulting material was expected to present adequate electrical properties and be able to be used in electrical equipment enclosures.

Materials and Methods

Raw Materials

The recycled ABS polymer was supplied by Sinctronics (Sorocaba, São Paulo State, Brazil), a reverse logistics innovation center for electrical and electronic equipment. The titanium dioxides used in this project were both commercial (COM) and modified surface (OPM). The former was purchased from Sigma-Aldrich (St. Louis, Missouri, USA) and named as Titanium (IV) oxide, in anatase form, and 99.8% purity, while the latter was synthesized and described in item 2.2. The metallic titanium (98%) was purchased from Sigma-Aldrich (St. Louis, Missouri, USA) and the H_2O_2/NH_3 was obtained from Synth (Brazil).

TiO_2 Surface Modification Method

TiO2-OPM was synthesized according to the methodology described by Nogueira et al. [13]. To produce TiO2-OPM, 250 mg of metallic titanium was added to 100 mL of H2O2/NH3 in a 3:2 proportion. The solution was inserted in an ice-water cooling bath until the complete dissolution of the metal was complete. The resultant solution showed a transparent-yellow color, corresponding to the peroxytitanate complex [14–16]. To form Ti(OH)4 with the surface modified by peroxo groups, the peroxytitanate complex solution was heated to 80 °C under stirring until the formation of a yellowish gel which was dried at 60 °C for 24 h. The TiO2-OPM was obtained with the calcination of Ti(OH)4 at 200 °C for 4 h at a heating rate of 10 °C/min.

Preparation of Modified r-ABS-TiO2

The raw materials were mixed using a ThermoScientific HAAKE PolyLab Rheomix QC (USA) equipment using 190 °C and 50 rpm as mixture settings, with the materials filling 70% of the mixture chamber's volume in a process that lasted nearly 8 min for each composite. These composites were produced in the proportions of 0.5, 1.0, and 3.0% of TiO_2, for both commercial and OPM. Samples are named as described in Table 1.

Evaluation of the Composite Properties

Titanium dioxide powders and composites were characterized by microscopy techniques such as scanning electron microscopy SEM (FEI Inspect S50, Germany). For the analysis, the samples were coated with a thin layer of gold, in a method known as *sputtering*.

X-ray diffraction (XRD) analysis was performed using Cu Kα radiation (Shimadzu X-Ray Diffractometer XRD-6000, Japan) in a 2θ range from 10° to 80°, with a 0.02° step scan.

Thermal characterization techniques were also used to evaluate the thermal stability, as well as the influence of modification on the degradative behavior of the polymer. Both differential scanning calorimetry (DSC) and dynamic

Table 1 Nomenclature of the samples used in this work

% of the Polymer matrix (ABS)	% of TiO2 particles	Nomenclature*
100	0	r-ABS
99.5	0.5	r-ABS 0.5% TiO_2
99.0	1.0	r-ABS 1% TiO_2
97.0	3.0	r-ABS 3% TiO_2

*TiO_2-COM and TiO_2-OPM to commercial and modified, respectively

oxidative induction temperature (OITD) were performed in a DSC NEZSTCH 203 F3-Maia equipment (Germany). For the DSC analysis, an N_2 atmosphere was used with a temperature range of 20–300 °C and a heating and cooling rate of 10 °C/min, while the dynamic OIT analysis occurred under an O_2 atmosphere, from 20 to 380 °C with a heating rate of 10 °C/min.

A thermogravimetric analysis (TGA) was performed on the materials with the intent to verify their behavior under high temperatures and an oxidizing atmosphere. It was performed in a TA Instruments TGA-Q50 (USA), with the temperature ranging from 40 to 700 °C, with an increase of 10 °C/min, using an O_2 atmosphere.

Dynamic mechanical analysis (DMA) was performed using a Dynamic Mechanical Analyzer Q800 from T.A. Instruments (USA) with a film tension clamp. The analyses were performed in cryogenic conditions, with a temperature range of − 70 to 170 °C, increasing by 2 °C/min. The tests were made at a 1 Hz frequency.

Infrared characterization was also used to examine raw materials and composites. The FTIR technique was performed with the ATR technique in the 4000 to 400 cm^{-1} range (ThermoScientific Nicolet 6700, USA).

Raman spectroscopy was performed with a Horiba Jobin–Yvon Raman microspectrometer LabRAM (Japan) at room temperature, using the 633 nm line of a 5.9 mW He–Ne laser as an excitation source and an Olympus TM BX41 microscope (Germany).

Rheological analyses were performed using parallel plates Modular Compact Rheometer MCR-302 from Anton Paar (Austria). The viscoelastic linear region (VELR) values were obtained from each sample by applying an increasing deformation, from 0.1 to 50%, using an angular frequency (ω) fixed at 1%, under an N_2 atmosphere and a temperature of 190 °C. Frequency Sweep analyses were then made following the shear strain value obtained by the VELR regimen. Samples were also analyzed under an N_2 atmosphere and a temperature of 190 °C. The shear strain (γ) used was fixed at 1%, and the angular frequency (ω) was diminished from 500 to 0.01 rad/s. The rheometer's rotational plate diameter was 25 mm and it was separated from the stationary plate by a 1 mm gap.

To investigate the electrical properties of the materials, they were subjected to a surface resistivity analysis using an ESD-800 equipment from ROHS. The analyses were performed using the two-probe method.

Two-probe Method

To perform the two-probe method [18], samples with a diameter of 5 cm ± 0.17 cm and thickness of 0.2–0.4 mm) and area (A) were used. For each sample, the measurement was performed in triplicate.

Voltage (V) and current flow (i) were monitored using a voltmeter, and a voltage source (DC) was used to generate current flow. The electrical resistivity (ρ) was calculated using Eq. 1.

$$\rho = \frac{VA}{id} \tag{1}$$

As is well known, there can be no current flow between two points of a material if there is no voltage difference in the applied potential between those points. In the internal circuit of the multimeter, there is a voltage source (DC), which is used to apply an electrical voltage to the material. The multimeter itself calculates (R = V/i) the electrical resistance of the sample.

Results and Discussion

Morphological and Structural Analysis of the Particles

Figure 1a, b shows the SEM images for the TiO_2 particles. Commercial titanium dioxide (Fig. 1a) has a more uniform distribution of morphology and size of its particles, with most of them in the nanometric range (100 nm). It is also visible that they tend to agglomerate. On the other hand, the TiO_2—OPM particles (Fig. 1b) lack uniformity in size and morphology. It seems that the particles are much larger than the nanometric scale. This lack of uniformity makes the material rich in defects that may contribute to charge redistribution and the presence of peroxo groups bonded to the surface of TiO2 particle enhanced reactivity relative to the commercial one. Furthermore, as previously analyzed by Francatto et al. [26] TiO2–OPM presents a short time needed to disperse the energy released during the exothermic decomposition of the peroxo groups. This increases its reactivity, which means there is enough local energy to activate the TiO2–OPM surface to react faster and at lower temperatures when compared to commercial ones. This is discussed by Ribeiro et al. [19], noting that the TiO_2-OPM powder is, in fact, smaller than commercial TiO_2 and, due to its small size–and therefore high surface energy–they form agglomerates with no defined morphology.

The XRD patterns of the TiO_2 and TiO_2-OPM are shown in Fig. 1c and give the structural information for the particles. Commercial titanium dioxide equals the diffractogram for the anatase phase, with its distinctive peaks at 2θ values of 25.62°, 38.16°, 48.44°, 54.27°, 55.45°, 63.02°, and 69.17°, representing the (101), (004), (200), (105), (211), (204) and (116) planes, shown in the image, as presented in the literature (ICDD No. 00-021-1272/COD 9008213 [20–22]).

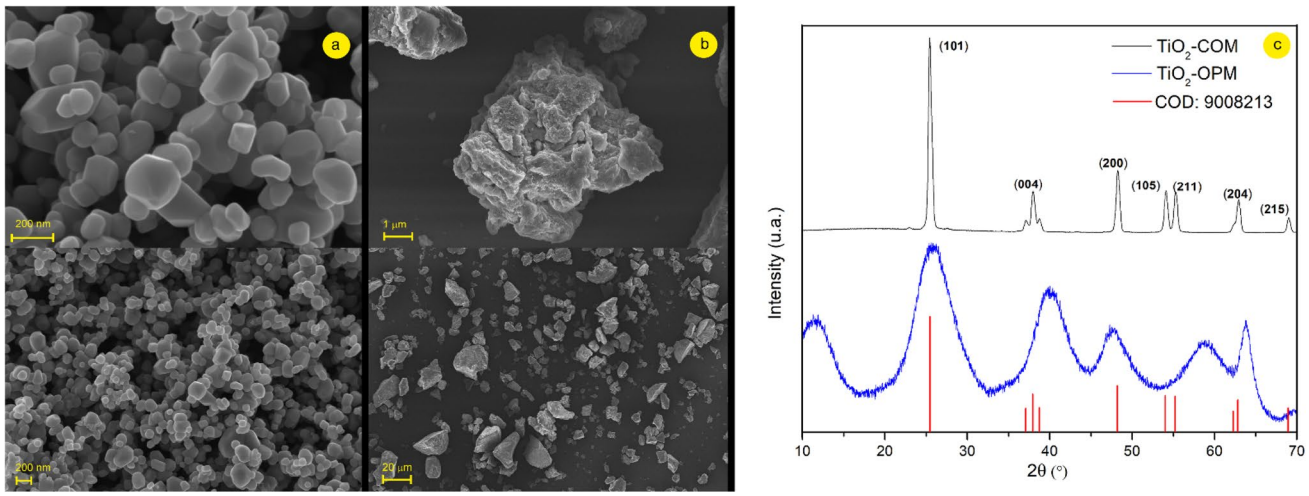

Fig. 1 **a** SEM microscopy of **a** commercial dioxide of titanium, **b** peroxo modified titanium dioxide, and **c** DRX patterns

The diffractogram for the OPM particles does not give an exact indication of its form. It shows their amorphous structure, with the smaller size of those particles being the reason for the pattern shown in the image. These results are corroborated by the aforementioned Ribeiro et al. work, especially for the TiO_2-OPM, where the same XRD pattern is observed.

The Effect of the Particle on Physicochemical ABS Properties

Figure 2a shows the XRD results for the r-ABS and its composites with 3% of both TiO_2. For the r-ABS, it is visible that there are peaks that are not present in the neat non-recycled ABS, according to the literature [23]. It is expected, though, as the r-ABS contains a vast number of additives in its composition, resulting in those peaks. For the diffractogram of the composites, it is shown that the incorporation of the particles gives the typical peaks for the anatase phase for either commercial or OPM titanium dioxide.

Figure 2b presents the FTIR spectra for the ABS and its composites. It is visible that no noticeable changes in its characteristic peaks were produced with the addition of the TiO_2 particles. The peaks from each ABS monomer are noted, with the butadiene's aliphatic CH bond shown at the 3050–2850 cm^{-1} region, along with a couple of peaks at the 970–910 cm^{-1} region, where the $CH{=}CH_2$ bond is noted. The sharp peak at 2235 cm^{-1} denotes the CN group existing

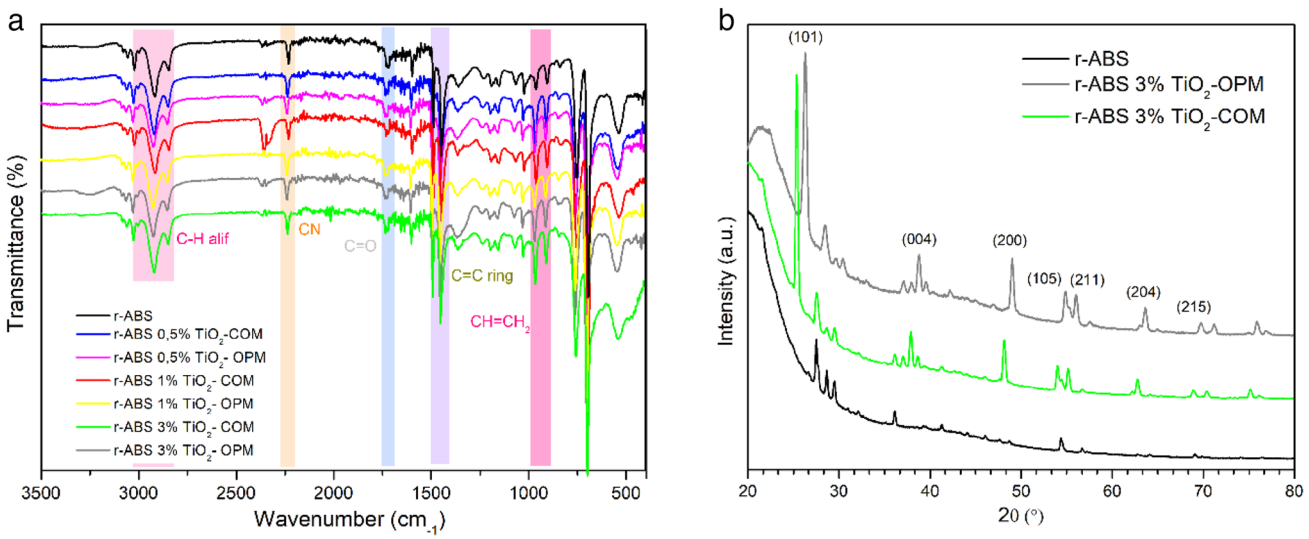

Fig. 2 **a** DRX patterns and **b** FTIR spectra of the composites

in the acrylonitrile monomer. The polystyrene presence is confirmed by the ring's C=C bond sharp peaks observed at the 1500–1400 cm^{-1} region, jointly with the aromatic CH bond peaks at the 700 cm^{-1} region. There is a peak at 1730 cm^{-1}, which denotes the C=O group. This could be intensified due to degradation processes suffered as the polymer is recycled. It can also be attributed to groups that exist in the carbon black additive that is also present in the recycled material. Furthermore, the incorporation of titanium dioxides did not cause changes in the region around 1000–400 cm^{-1} where a broad peak was expected, as it is a characteristic peak for the anatase TiO_2.

Effect of the Modification of ABS on the Thermal/Degradation Properties

The DSC and DMA curves for the samples of r-ABS and its composites were illustrated in Fig. 3a, b, respectively. The glass transition temperature (Tg) for the materials obtained by both techniques is present in Fig. 3. The results obtained by DSC were practically unchanged. This is probably because the addition of particles did not significantly change the mobility of the amorphous phase. However, the Tg values obtained by the DMA analysis show a tendency to be superior for the composites when compared to pristine ABS. The ABS is a blend of two random copolymer–poly(acrylonitrile-*stat*-butadiene), SAN phase, and poly(butadiene), phase PB and, as described by Algadhi et al. [24], the phase PB presents a Tg lower than − 90 °C, that means the Tg present in Fig. 3 is associated with SAN phase.

The DMA analysis is more precise than the DSC as a means of obtaining the Tg values, as stated by Foreman et al. [25]. From the results presented in Fig. 3 an increase in Tg (SAN phase) is observed indicating a possible polymeric matrix-particle interaction.

Although inorganic materials are widely used to improve properties, especially thermal and mechanical ones, they can often induce degradative processes in the polymeric matrix. And few works in literature have been devoted to studying this aspect. Considering this context, a detailed investigation of the thermal behavior of this

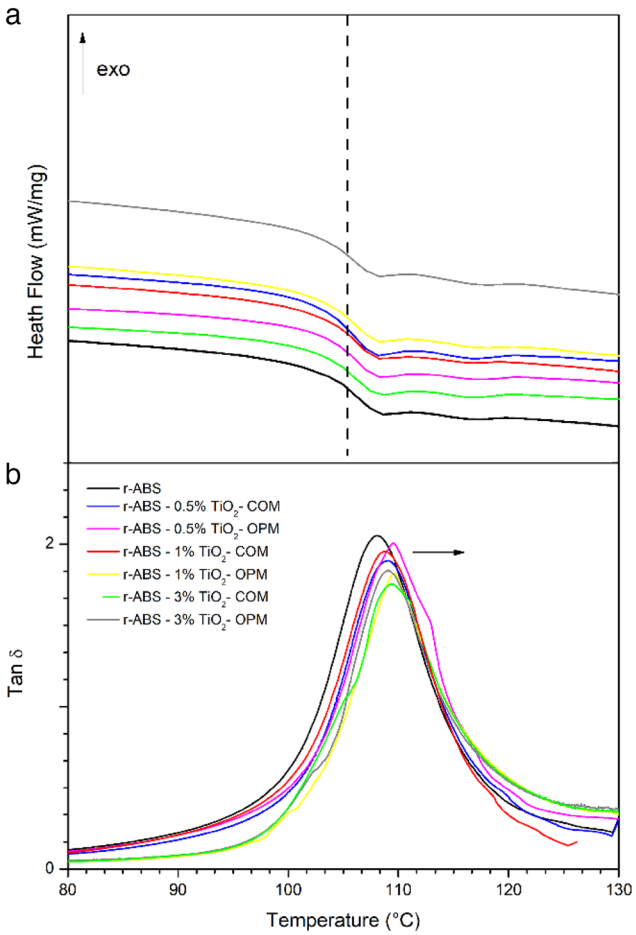

c

Amostra	DSC Tg (°C)	DMTA Tg (°C)
r-ABS	103 ± 1	108
r- ABS 0.5% TiO_2 - COM	103 ± 0	109
r- ABS 0.5% TiO_2 - OPM	103 ± 1	110
r- ABS 1% TiO_2 - COM	104 ± 1	109
r- ABS 1% TiO_2 - OPM	103 ± 1	112
r- ABS 3% TiO_2 - COM	103 ± 1	113
r- ABS 3% TiO_2 - OPM	102 ± 2	113

Fig. 3 **a** DSC curves and, **b** DMA curves for the composites indicating the Tg of SAN phase

system was done, and dynamic OIT, as well as TGA analyses, were performed (Fig. 4). A more in-depth look at this discussion can be given by analyzing the mechanisms of ABS degradation (Fig. 5).

The first exothermic event, Fig. 4a, represents the thermo-oxidation of the butadiene phase, where, under the effect of heat, the carbon bond adjacent to the double bond is broken, resulting in radical species that are attacked by the O_2 present in the sample. The second event starts around 320 °C and represents the SAN (styrene/acrylonitrile) phase degradation. The sequence of events can be explained by analyzing Fig. 5, which presents a proposed mechanism for ABS degradation.

The event for the r-ABS follows a smooth curve, while the composites produce several peaks that can be attributed to the effect of the particles in the way degradation occurs. Those particles can influence the path of degradation of the SAN phase, slowing it or giving different degradation subproducts in the process. These values are presented in Table 2 in the form of the onset temperature (T_{onset}), the temperature at which the technique detects the beginning of a degradation process for both phases.

As described previously, peroxo groups are quite unstable, which can result in their decomposition at lower temperatures, catalyzing the degradation reactions of the butadiene phase. Releasing around 305 J/g [19], the decomposition of peroxo groups bonded to TiO_2 leads to an exothermic decomposition, where the local energy needed to activate the nanoparticle surface is enough to make the reaction go faster at lower temperatures, approaching an adiabatic transformation. Peroxides can decrease the energy barrier during the solid-state reaction due to the increase of the chemical bond's lability near central titanium making the diffusion of atoms at lower temperatures and shorter times [26].

Both the presence of commercial TiO_2-COM and TiO_2-OPM affect oxidative stability at low concentrations. At higher concentrations, an antagonistic effect is observed. Concentrations of 3% commercial TiO_2 shows an increase in thermal stability, but the modified TiO_2 (r-ABS 3% TiO_2-OPM) appears to catalyze the degradation reactions. It is observed for the SAN phase an increase in the temperature for the beginning of the oxidative reactions in both cases. The results may be supported by analyzing Fig. 5, which shows a proposal for a mechanism scheme for these

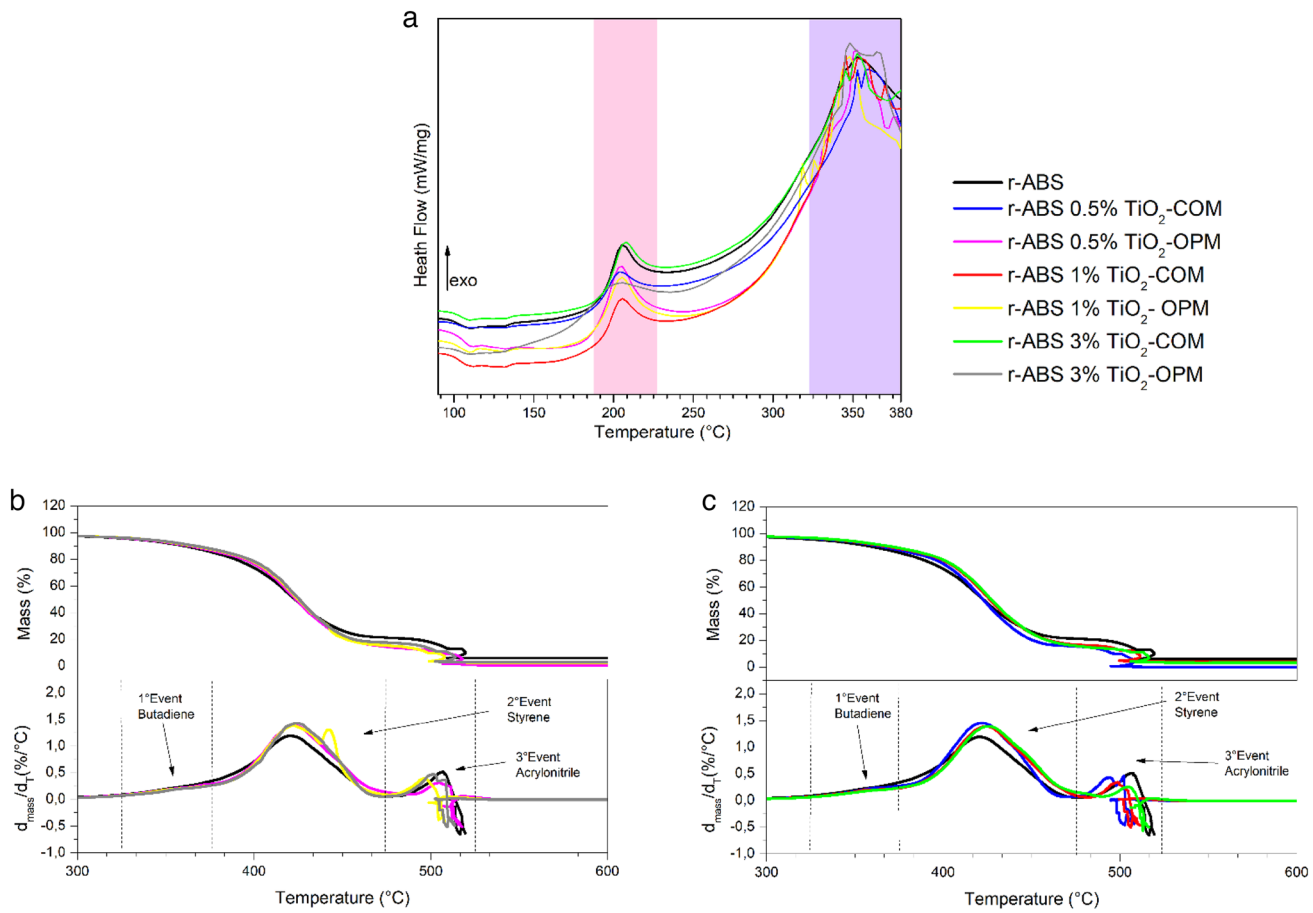

Fig. 4 **a** OITD, **b** TGA curves for ABS-TiO_2-COM, and **c** ABS-TiO_2-OPM

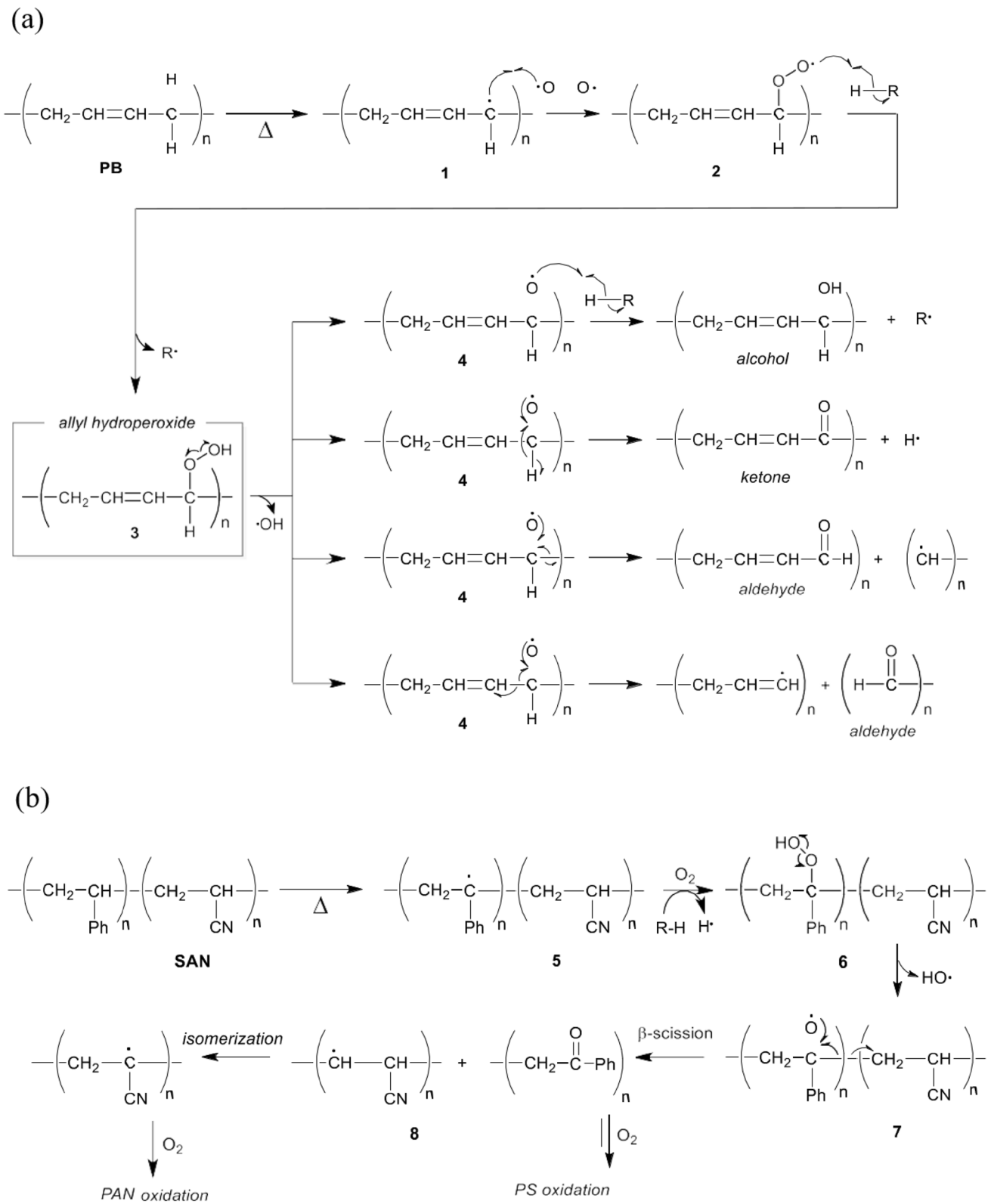

Fig. 5 Proposed mechanism for ABS degradation: **a** PB phase, and **b** SAN phase

Table 2 Temperatures for the degradation events observed in the dynamic OIT

Polymer/composite	Texo (°C) (PB)	Texo (°C) (SAN)
r-ABS	190	284
r-ABS 0.5% TiO2-COM	184	282
r-ABS 1% TiO2-COM	187	282
r-ABS 3% TiO2-COM	190	279
r-ABS 0.5% TiO2-OPM	184	282
r-ABS 1% TiO2-OPM	187	283
r-ABS 3% TiO2-OPM	155	274

degradation events. In the initiation step of the PB phase, high temperatures easily promote C-H bond homolytic cleavage in the secondary allylic position producing free allyl radicals which are resonance-stabilized by a double bond (**1**) (Fig. 5a). The second stage involves the reaction between the allyl radical **1** with molecular oxygen and the formation of the peroxy radical **2.** The abstraction of hydrogen atoms of these peroxy radicals from the carbon chain (R-H) gradually accumulate hydroperoxide **3**. These hydroperoxides can trigger a sequence of events after thermal decomposition and formation of the alkoxy radical **4**, inducing autoxidation of the PB phase. Alcohols are produced from alkoxy radical **4** by the abstraction of a hydrogen atom. Alternatively, the formation of carbonyls (ketones and aldehydes) can easily be formed after a process called β-scission or β-fragmentation of alkoxy radicals **4** [27].

A similar sequence of events could explain the damage to the polymeric chain of the SAN phase under a severe thermal oxidative condition (Fig. 5b). Heat-induced chain-scission of SAN grafts occur via homolytic cleavage, forming resonance-stabilized benzylic radicals **5** that in the presence of oxygen, undergo oxidative processes, as described in Fig. 5b. After formation of hydroperoxides **6** and thermal decomposition, alkoxy radical induce autoxidation of the PS *mers*. On the other hand, the primary free radical PAN fragment **8** from the SAN phase can undergo an isomerization process, forming a more stable tertiary and benzylic radical, which can be oxidized during more severe degradation stages [28].

A TGA analysis was performed (Fig. 4) to further investigate the degradative processes suffered by the materials. In literature, it is described that there are three main events in ABS thermal decomposition in the presence of oxygen in TGA: (1) the first one is around 340 °C, related to butadiene; (2) the second is around 420 °C, where styrene phase becomes more important, and the last one (3) that starts in 400 °C and ceases by 450 °C showing the evolution of the decomposition of acrylonitrile [29]. Table 3 shows the events for all samples obtained from the TGA analysis under an oxygen atmosphere. The first event concerning butadiene is quite subtle for both TiO_2-COM and TiO_2-OPM, indicating negligible mass loss.

The butadiene phase is present in a smaller amount. Thus, the analysis of its stability was determined when the mass loss is associated with 5% (T_{95}–Table 3). The presence of the TiO_2-OPM particles results in a reduction of the temperature for the initiation of the degradation of the butadiene phase. The degradation step described in the proposed mechanism (Fig. 5) indicates that this phase can be initially degraded with the contribution of TiO_2-OPM. This fact is corroborated by the reduction in temperature for the initiation of oxidation reactions of this phase (Fig. 4). Although no significant change in T_{max} of the polystyrene phase (T_{max1}) is observed, the degradation kinetics (ΔT_{max1}) concerning the PB phase is slower, especially with the incorporation of TiO2- OPM. This fact was already expected since the initiation for decomposition occurs at lower temperatures. The same behavior is observed for the acrylonitrile phase concerning degradation kinetics. However, an increase in T_{max2} for this phase is observed. The particle was hypothesized to act as a physical barrier that prevents the release of volatiles. Comparatively, Fitaroni et al. observed similar behavior on the influence of montmorillonite clay on the thermal stability of PP [30]. The results presented indicated that the Ti values

Table 3 Events observed with TGA analysis for the samples

Polymer/composite	T_{95}* (°C)	T_{max1} (°C)	T_{max2} (°C)	ΔT_{max1} (°C)	ΔT_{max2} (°C)
r-ABS	340.5 ± 0.7	420.0 ± 2.8	493.0 ± 8.8	79.5 ± 2.1	152.5 ± 7.8
r-ABS 0.5% TiO2-COM	339.5 ± 0.7	422.5 ± 0.7	495.5 ± 4.3	83.0 ± 1.4	156.0 ± 4.2
r-ABS 1% TiO_2-COM	338.0 ± 7.1	422.5 ± 2.1	500.0 ± 1.7	84.5 ± 4.9	162.0 ± 8.5
r-ABS 3% TiO_2-COM	339.5 ± 4.9	424.0 ± 1.4	505.0 ± 1.9	84.5 ± 3.5	165.5 ± 6.4
r-ABS 0.5% TiO_2-OPM	334.0 ± 1.4	421.0 ± 1.4	503.5 ± 1.7	87.0 ± 0	169.5 ± 0.7
r-ABS 1% TiO_2-OPM	334.5 ± 3.5	421.0 ± 1.4	501.0 ± 5.9	86.5 ± 2.1	166.5 ± 9.2
r-ABS 3% TiO_2-OPM	334.5 ± 3.5	422.0 ± 2.8	504.0 ± 4.0	87.5 ± 0,7	169.5 ± 7.8

*T_{95} indicates that the samples lose 5% of the initial mass, T_{max1} is associated with the maximum speed mass loss temperature of the styrene phase, T_{max2} is associated with the maximum speed mass loss temperature of the acrylonitrile phase and, ΔT represents the difference between T_{max} and T_{95}

did not change significantly, but an increase in Tmax was observed with increasing clay content.

The increase in ΔT observed indicate that the presence of particles alters the internal structure of the polymer in a way that hinders the production of volatiles. This behavior is clearer for samples with TiO_2-OPM, again signaling that a good interaction occurs between particle and polymer. Additionally, an increase in the mean free path for oxygen entry and volatile exit due to the presence of particles can be observed, meaning slower gas diffusion inside the polymer matrix.

Rheological Analysis

To evaluate the interaction between the particles and the polymeric matrix, rheological tests were performed in an oscillatory regimen and information on the complex viscosity and storage and loss modules were obtained (Fig. 7). At lower frequencies, it is possible to see that there is an increase in the complex viscosity values with the particle incorporation, except for the composites with 0.5% TiO_2, which indicates a good particle/polymer interaction, as verified by thermal analysis. As the frequency increases, these values tend to converge to approximate values. In this high-frequency condition, the polymeric chains cannot return to their natural state of entanglement, acquiring more fluidity and consequently being less dependent on the particle presence. They are more frequency-dependent than particle concentration.

Analyzing the storage modulus (G') and loss modulus (G"), in Fig. 6b, c is seen that at higher frequencies the G' value is higher than G". This information indicated that the material has a solid-like behavior. As the frequency decreases, there is an inversion of these values, where G" > G', and the material begins to show liquid-like behavior. But then again, at lower frequencies, this pattern changes

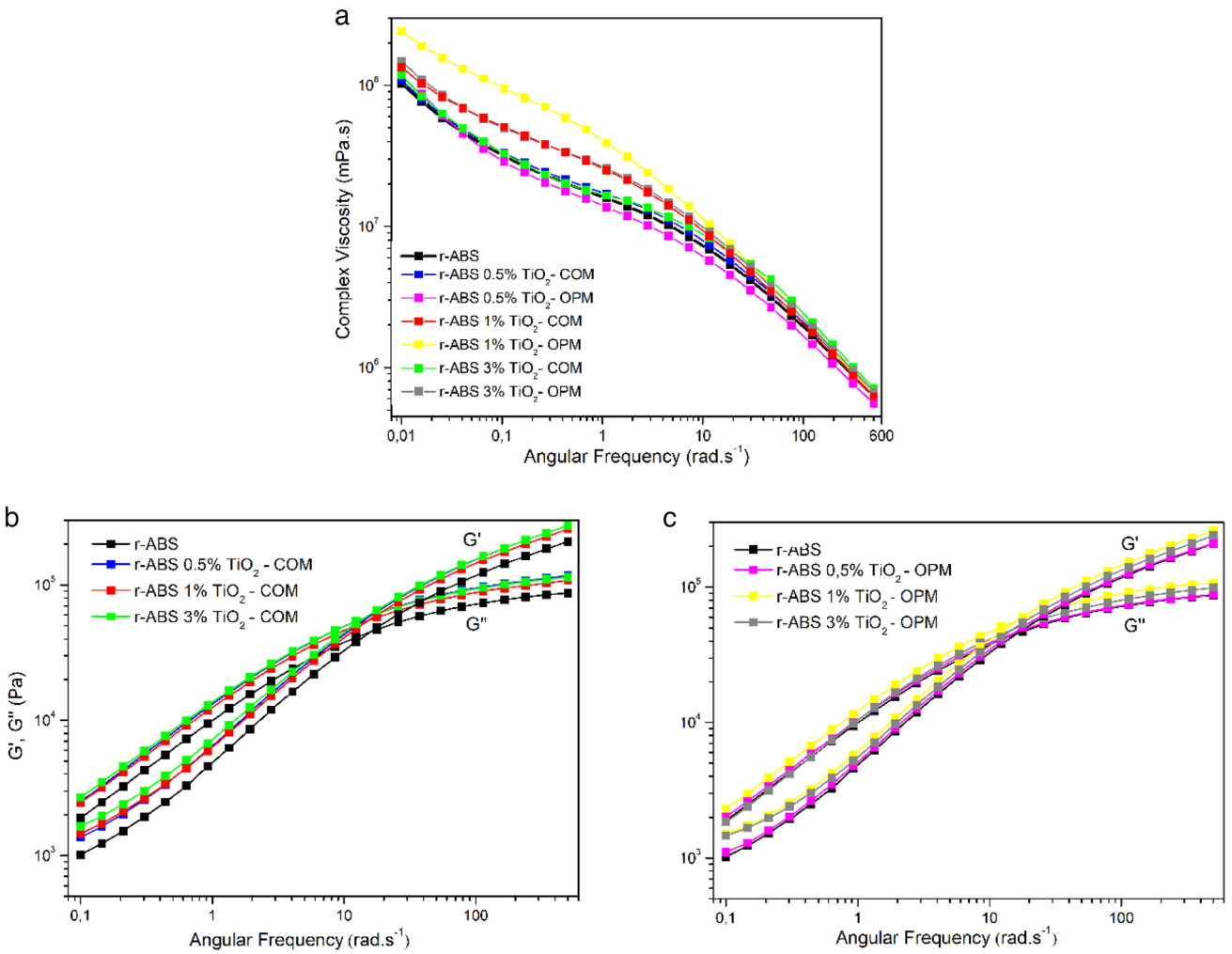

Fig. 6 **a** Complex viscosity, storage modulus (G') and loss modulus (G") to samples modified with **b** TiO_2–COM and, **c** TiO_2–OPM as a function of frequency

Table 4 Surface resistivity values for the samples

Polymer/composite	Surface resistivity (Ω/sq)	ESD Classification
r-ABS	$(4.59 \pm 0.46) \cdot 10^{10}$	Antistatic
r-ABS 0.5% TiO2-COM	$(3.92 \pm 1.13) \cdot 10^{10}$	Antistatic
r-ABS 1% TiO2-COM	$(3.97 \pm 0.26) \cdot 10^{10}$	Antistatic
r-ABS 3% TiO2-COM	$(2.92 \pm 0.39) \cdot 10^{10}$	Antistatic
r-ABS 0.5% TiO2-OPM	$(4.11 \pm 2.53) \cdot 10^{7}$	Dissipative
r-ABS 1% TiO2-OPM	$(8.04 \pm 0.11) \cdot 10^{6}$	Dissipative
r-ABS 3% TiO2-OPM	$(8.69 \pm 0.88) \cdot 10^{5}$	Dissipative

again, and G' surpasses G". This profile indicates the interaction between polymer/particles and denotes the tendency for the formation of a percolation network.

Electrical Analysis

To verify the influence of TiO_2 particles on the electrical properties of the polymer, especially on the antistatic properties, surface resistivity tests were performed, and the results are presented in Table 4. Given the need for good protection against electrostatic discharges for their use in electronic equipment, they are classified according to their ability to avoid such discharges. Inherently, polymers are insulators, meaning that they cannot dissipate the cumulative charges on their surface, leading eventually to their discharge. The manufacture of composites through the incorporation of particles that have good electrical conductivity can lead to a better ability to handle such charges and prevent electrostatic discharges. Thus, as the results show, the r-ABS no longer is classified as an insulator due to the presence of carbon black, a known additive that is capable to enhance the polymer conductivity. Carbon black is an additive typically employed in the electronics industry, and post-consumer recycled material (ABS-r) has this additive in its composition. It is classified as an antistatic, meaning that it has a slightly better capacity to dissipate the charges. Commercial TiO_2 composites fall in the same classification, meaning that this particle is not capable of changing the electrical properties presented by the r-ABS alone.

This is drastically changed for the composites containing TiO_2-OPM particles. They fall into the *dissipative* classification because their surface resistivity values were greatly diminished, even for the lowest percentage of titanium dioxide incorporation–0.5%. However, it was expected, as indicated by the difference in band gap values for the TiO_2 powders. With a lower band gap value, the OPM powder was expected to have better electrical conductivity, and its incorporation within the polymeric matrix would increase the overall electrical conductivity of the resulting composite, and this is proven true.

Conclusions

In this work, ABS from waste electrical and electronic equipment was recycled using TiO_2 modified with peroxo groups. The reintroduction of this material to the same production cycle depends, among several aspects, on adequate viscosity/fluidity and antistatic properties. The lower band gap of TiO_2-OPM particles, when compared to commercial TiO_2, associated with a good dispersive and distributive mixing led to materials with dissipative properties even at low particle concentrations. Rheological data indicates the interaction between polymer/particles and denotes the tendency for the formation of a percolation network.

An in-depth investigation of the degradative processes and their relationship with the presence of OPM in the TiO_2 particle was carried out. The peroxo groups catalyzed the degradation reactions of the butadiene due to lower stability. Despite this, its impact on the complex viscosity/molar mass is not observed, which can be explained by the fact that this phase is mostly smaller—in composition—and the eventual decrease in molar mass is compensated by the interactions described above.

Additionally, the TGA results led to two main findings with the incorporation of the particle modified with OPM: (a) the degradation of the butadiene phase occurs at lower temperatures, (b) those of the styrene and acrylonitrile phase at higher temperatures (probably the difficulty of volatiles output by the increase in the free mean path), and additionally to this effect (c) the degradation kinetics is slower.

Finally, it is possible to conclude that the incorporation of surface-modified TiO_2 into the r-ABS polymeric matrix provided an efficient way to enhance the antistatic characteristic of the material, allowing its use in electronic equipment. Furthermore, it has been shown that a recycled polymer can be reintroduced into the market with the desired properties by manufacturing a composite with it.

Author Contributions SAC—responsible for the ideation and conception of the work, as well as for the promotion and discussion at all stages. IMO—executed, discussed, and wrote most of the work. JCFG and MABF—both are responsible for the discussion and design of the organic reactions. CMPS and ERC—developed the particles. GX—did the DMA analysis.

Funding The authors would like to thank the financial funding given by the Coordination of Higher Education Personnel – CAPES. This work was funded in part by Fundação de Amparo à Pesquisa do Estado de São Paulo - FAPESP CEPID-finance code 2013/07296-2.

Availability of Data and Material All data are in the authors' domain and can be requested as soon as the journal requests.

Declarations

Conflict of Interest The authors confirm that they have no conflicts of interest concerning the work described in this manuscript.

References

1. C. Bastioli (2005) Handbook of Biodegradable Polymers, Rapra Technology Limited, Shawbury.
2. Ramesh V, Biswal M, Mohanty S, Nayak SK (2014) Recycling of engineering plastics from waste electrical and electronic equipments: influence of virgin polycarbonate and impact modifier on the final performance of blends. Res Waste Manag. https://doi.org/10.1177/0734242X14528404
3. Beigbeder J, Perrin D, Mascaro JF, Lopez-Cuesta JM (2013) Study of the physico-chemical properties of recycled polymers from waste electrical and electronic equipment (WEEE) sorted by high resolution near infrared devices. Resour Conserv Recycl. https://doi.org/10.1016/j.resconrec.2013.07.006
4. Liu X, Lu X, Feng Y, Zhang L, Yuan Z (2022) Recycled WEEE plastics in China: generation trend and environmental impacts. Resour Conserv Recycl. https://doi.org/10.1016/j.resconrec.2021.105978
5. Signoret C, Girard P, Le Guen A, Caro-bretelle AS, Lopez-cuesta JM, Ienny P, Perrin D (2021) Degradation of styrenic plastics during recycling: accommodation of pp within abs after weee plastics imperfect sorting. Polymers (Basel). https://doi.org/10.3390/polym13091439
6. Chaine C, Hursthouse AS, McLean B, McLellan I, McMahon B, McNulty J, Miller J, Viza E (2022) Recycling plastics from WEEE: a review of the environmental and human health challenges associated with brominated flame retardants. Int J Environ Res Public Health. https://doi.org/10.3390/ijerph19020766
7. Maisel F, Chancerel P, Dimitrova G, Emmerich J, Nissen NF, Schneider-Ramelow M (2020) Preparing WEEE plastics for recycling—how optimal particle sizes in pre-processing can improve the separation efficiency of high quality plastics. Resour Conserv Recycl. https://doi.org/10.1016/j.resconrec.2019.104619
8. Gómez M, Peisino LE, Kreiker J, Gaggino R, Cappelletti AL, Martín SE et al (2020) Stabilization of hazardous compounds from WEEE plastic: development of a novel core-shell recycled plastic aggregate for use in building materials. Constr Build Mater. https://doi.org/10.1016/j.conbuildmat.2019.116977
9. Wagner F, Peeters JR, De Keyzer J, Janssens K, Duflou JR, Dewulf W (2019) Towards a more circular economy for WEEE plastics—Part A: development of innovative recycling strategies. Waste Manag. https://doi.org/10.1016/j.wasman.2019.09.026
10. Cesaro A, Marra A, Belgiorno V, Guida M (2017) Effectiveness of WEEE mechanical treatment: separation yields and recovered material toxicity. J Clean Prod 142:2656–2662. https://doi.org/10.1016/j.jclepro.2016.11.011
11. Vazquez YV, Barbosa SE (2016) Recycling of mixed plastic waste from electrical and electronic equipment. Added value by compatibilization. Waste Manag. https://doi.org/10.1016/j.wasman.2016.04.022
12. Kopnina H, Padfield R (2021) Environmental and sustainability indicators (Im) possibilities of "circular" production: learning from corporate case studies of (un) sustainability. Environ Sustain Indic. https://doi.org/10.1016/j.indic.2021.100161
13. Tamoor M, Samak NA, Yang M, Xing J (2022) The cradle-to-cradle life cycle assessment of polyethylene terephthalate: environmental perspective. Molecules. https://doi.org/10.3390/molecules27051599
14. Ghiţă B, Helerea E (2016) Qualification of polymeric compounds for electrostatic discharge protection. Int Conf Appl Theor Electr ICATE. https://doi.org/10.1109/ICATE.2016.7754657
15. Brabazon D (2021) Introduction: Polymer Matrix Composite Materials. Mater. Compos, Encycl. https://doi.org/10.1016/b978-0-12-819724-0.00109-9
16. Dahman SJ (2023) All polymeric compounds: conductive and dissipative polymers in ESD control materials. Electr Overstress/Electrost Disch Symp Proc 2003–459:1–7
17. Nogueira AE, Longo E, Leite ER, Camargo ER (2014) Synthesis and photocatalytic properties of bismuth titanate with different structures via oxidant peroxo method 462(OPM). J Colloid Interface Sci. https://doi.org/10.1016/j.jcis.2013.10.010
18. Singh Y (2013) Electrical resistivity measurements: a review. Int J Mod Phys Conf Ser. https://doi.org/10.1142/s2010194513010970
19. Ribeiro LS, Nogueira AE, Aquino JM, Camargo ER (2019) A new strategy to obtain nano-scale particles of lithium titanate (Li4Ti5O12) by the oxidant peroxo method (OPM). Ceram Int. https://doi.org/10.1016/j.ceramint.2019.07.274
20. Merkys A, Vaitkus A, Grybauskas A, Konovalovas A, Quirós M, Gražulis S (2023) Graph isomorphism-based algorithm for cross-checking chemical and crystallographic descriptions. J Cheminform. https://doi.org/10.1186/s13321-023-00692-1
21. Vaitkus A, Merkys A, Gražulis S (2021) Validation of the crystallography open database using the crystallographic information framework. J Appl Crystallogr. https://doi.org/10.1107/S1600576720016532
22. Quirós M, Gražulis S, Girdzijauskaitė S, Merkys A, Vaitkus A (2018) Using SMILES strings for the description of chemical connectivity in the crystallography open database. J Cheminform. https://doi.org/10.1186/s13321-018-0279-6
23. Olongal M, Raphael LR, Raghavan P, Nainar MAM, Athiyanathil S (2021) Maleic anhydride grafted acrylonitrile butadiene styrene (ABS)/zinc oxide nanocomposite: an anti-microbial material. J Res Polym. https://doi.org/10.1007/s10965-021-02632-9
24. Alghadi AM, Tirkes S, Tayfun U (2020) Mechanical, thermo-mechanical and morphological characterization of ABS based composites loaded with perlite mineral. Mater Res Express. https://doi.org/10.1088/2053-1591/ab551b
25. Foreman J, Sauerbrunn SR, Marcozzi CL (1997) Exploring the sensitivity of thermal analysis techniques to the glass transition, TA instruments. https://www.tainstruments.com/pdf/literature/TA082.pdf. Accessed 15 Jun 2023
26. Francatto P, Souza Neto FN, Nogueira AE, Kubo AM, Ribeiro LS, Gonçalves LP, Gorup LF, Leite ER, Camargo ER (2016) Enhanced reactivity of peroxo- modified surface of titanium dioxide nanoparticles used to synthesize ultrafine bismuth titanate powders at lower temperatures. Ceram Int. https://doi.org/10.1016/j.ceramint.2016.07.039
27. Shimada J, Kabuki K (1968) The mechanism of oxidative degradation of ABS resin. Part I. The mechanism of photooxidative degradation. J Appl Polym Sci. https://doi.org/10.1002/app.1968.070120406
28. Mailhot B, Gardette JL (1994) Mechanism of poly(styrene-co-acrylonitrile) photooxidation. Polym Degrad Stab. https://doi.org/10.1016/0141-3910(94)90168-6
29. Suzuki M, Wilkie CA (1995) The thermal degradation of acrylonitrile-butadiene-styrene terpolymei as studied by TGA/FTIR. Polym Degrad Stab. https://doi.org/10.1016/0141-3910(94)00122-0

30. Fitaroni LB, De Lima JA, Cruz SA, Waldman WR (2015) Thermal stability of polypropylene-montmorillonite clay nanocomposites: limitation of the thermogravimetric analysis. Polym Degrad Stab. https://doi.org/10.1016/j.polymdegradstab.2014.10.016